Acta Materialia 123 (2017) 167–176

Contents lists available at ScienceDirect

Acta Materialia

journal homepage: www.elsevier.com/locate/actamat

Full length article

Atomic scale imaging of structural variations in $La_{(1-x)/3}Li_xNbO_3$ ($0 \leq x \leq 0.13$) solid electrolytes

Xiaobing Hu [a], Shunsuke Kobayashi [a], Yumi H. Ikuhara [a], Craig A.J. Fisher [a], Yasuyuki Fujiwara [b], Keigo Hoshikawa [b], Hiroki Moriwake [a], Keiichi Kohama [c], Hideki Iba [c], Yuichi Ikuhara [a, d, *]

[a] Nanostructures Research Laboratory, Japan Fine Ceramics Center, Nagoya 456-8587, Japan
[b] Faculty of Engineering, Shinshu University, Nagano 380-8553, Japan
[c] Battery Materials Division, Toyota Motor Corporation, Susono 410-1193, Japan
[d] Institute of Engineering Innovation, The University of Tokyo, Tokyo 113-8586, Japan

ARTICLE INFO

Article history:
Received 14 August 2016
Received in revised form
4 October 2016
Accepted 10 October 2016

Keywords:
Solid-state Li-ion battery
Solid electrolyte
Layered perovskite
Scanning transmission electron microscopy
Structure-property relationships

ABSTRACT

Solid-state Li-ion battery electrolyte materials $La_{(1-x)/3}Li_xNbO_3$ (LLNbO) are layered A-site-deficient perovskites with complex structural features resulting from their high intrinsic cation vacancy concentrations. We report an atomic-scale study of a series of single crystals of LLNbO with Li contents $x = 0$, 0.04, 0.07, and 0.13 using state-of-the-art scanning transmission electron microscopy. By combining high angle annular dark field and annular bright field imaging techniques, columns of heavy and light atoms could be imaged simultaneously with atomic resolution. Structure modulation within La-rich layers, observed in all samples, was strongest for Li content $x = 0.07$, the content which has been reported to exhibit the highest conductivity. Unlike for end member $La_{1/3}NbO_3$ ($x = 0$), for Li content $x = 0.04$, significant tilting of NbO_6 octahedra occurs, with regions of different tilting directions corresponding to nanodomains within the crystal. This tilting and the associated nanodomains are absent when $x = 0.07$, but occur again when $x = 0.13$, with even greater distortion of NbO_6 octahedra. These structural differences help explain the changes in Li-ion conductivity with Li content in LLNbO.

1. Introduction

In solid-state Li-ion batteries (SSLIBs), the organic Li-conducting electrolyte typically used in commercial Li-ion batteries is replaced with a solid-state Li-ion conductor. This provides a number of advantages, such as greater safety, wider thermal stability range, better shock and vibration resistance, less packaging material requirements, and easier materials handling [1–4]. For SSLIBs to be practicable, however, materials with higher Li-ion conductivities and improved cycling performance need to be developed that are also electronically insulating and stable in contact with suitable electrode materials [1,4,5]. One group of promising solid-state Li-ion conductors comprises A-cation deficient perovskites such as $La_{(2-x)/3}Li_xTiO_3$ (LLTO) [6–10] and $La_{(1-x)/3}Li_xNbO_3$ (LLNbO) [11–14]. In the case of LLTO, bulk Li-ion conductivities as high as 10^{-3} S.cm^{-1} have been achieved for $x \approx 0.11$ at room temperature.[6] Unfortunately, during battery charging, Ti^{4+} is easily reduced to Ti^{3+}, introducing electronic charge carriers that make LLTO materials unsuitable for use as electrolytes in SSLIBs [7]. LLNbO, on the other hand, remains electronically insulating during charge-discharge cycling, but reported Li-ion conductivities are an order of magnitude smaller than those of LLTO [11,12].

The $x = 0$ end member of the LLNbO series, $La_{1/3}NbO_3$, has the highest concentration of cation vacancies, twice that of $La_{2/3}TiO_3$. Rather than being randomly distributed over perovskite A sites, however, La atoms partition into alternating La-rich (average site occupancy factor = 2/3) and La-empty (site occupancy factor = 0) layers, labeled A1 and A2, respectively, along one axis. The X-ray diffraction (XRD) spectrum of $La_{1/3}NbO_3$ can be indexed to orthorhombic space group *Cmmm*, with $a = 7.82$ Å, $b = 7.84$ Å, and $c = 7.91$ Å at room temperature [15]. The (average) crystal structure is illustrated in Fig. 1.

Gradual replacement of La with Li (3 mol Li for 1 mol La) systematically alters the average structure. XRD analysis reveals a

* Corresponding author. Institute of Engineering Innovation, The University of Tokyo, Tokyo 113-8586, Japan.
E-mail address: ikuhara@sigma.t.u-tokyo.ac.jp (Y. Ikuhara).

http://dx.doi.org/10.1016/j.actamat.2016.10.025
1359-6454/

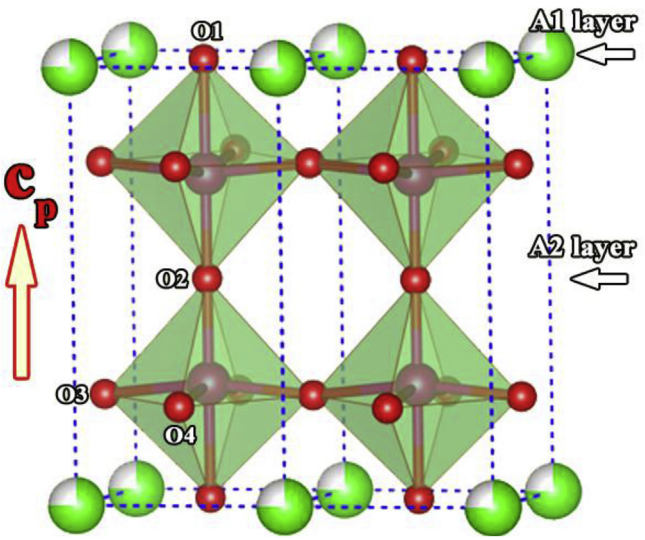

Fig. 1. Average crystal structure of layered perovskite $La_{1/3}NbO_3$. The green/white, pink, and red balls represent La atoms/vacancies, Nb atoms, and O atoms, respectively. The alternating partially occupied and unoccupied cation layers parallel to the *c* axis are labeled A1 and A2, respectively. O1, O2, O3 and O4 indicate the four symmetrically non-equivalent O sites. Blue dotted lines indicate double-perovskite units. (For interpretation of the references to colour in this figure legend, the reader is referred to the web version of this article.)

change from orthorhombic to tetragonal symmetry and finally to pseudo-cubic symmetry as Li content is increased from $x = 0$ to 0.25 [16]. As with LLTO, the Li-ion conductivity is also known to vary with Li content in LLNbO. The highest Li-ion conductivity in this system reported to date for polycrystalline samples is around 4.7×10^{-5} S.cm^{-1} at room temperature [11,16]. Replacing some La with Sr has also been reported to improve the Li-ion conductivity (7.3×10^{-5} S.cm^{-1} at 25 °C) [16,17]. Single crystals of LLNbO have even higher Li-ion conductivities, indicating that grain boundaries impede Li-ion diffusion, as was found for LLTO [18–20]. For example, by preparing single crystals of LLNbO by a directional solidification method the Li-ion conductivity could be doubled to around 1.9×10^{-4} S.cm^{-1} at 25 °C [21]. Other structural features, such as domain boundaries, dislocations, and defect clusters, are also known to affect ion conductivity in highly defective oxides [22,23]. It is thus important to investigate the crystal structure of LLNbO at the atomic level in order to develop strategies for optimizing its Li-ion conductivity. Today, high spatial resolution electron microscopy and related techniques make it possible to examine important nanostructural and microstructural features at the atomic level [24,25], and recent studies of a number of Li-ion conducting materials have demonstrated the usefulness of such methods [26–33].

Earlier studies of LLNbO using conventional transmission electron microscopy (TEM) methods such as selected area electron diffraction (SAED) and high resolution TEM (HRTEM) have indicated that the structures of these materials are much more complex than the average structure suggests, exhibiting domain formation and/or structure modulation as a function of Li content [11]. Direct visualization of atom columns within grains of LLNbO thin films using high angle annular dark field (HAADF) scanning transmission electron microscopy (STEM) has since confirmed the quasi-ordering of La in the A1 layers, corresponding to structure modulation, when viewed along the $[110]_p$ (where p refers to the pseudo-perovskite unit cell) direction [34].

Under the right conditions, annular bright field (ABF) STEM also makes it possible to image light elements such as H, O and Li, together with heavier elements [25]. Determining the positions of O atoms is particularly important in the case of LLNbO because it is directly related to the amount of local tilting/distortion of the NbO_6 octahedra, which alters the size of the bottlenecks through which Li ions must pass. Here we present a detailed investigation of LLNbO crystals with different Li content based on results of atomic resolution HAADF and ABF STEM imaging techniques. The electronic structure of LLNbO is also investigated using spatially resolved electron energy loss spectrometry (EELS) with high energy resolution.

2. Experimental section

2.1. Specimen preparation

Single crystals of composition $La_{(1-x)/3}Li_xNbO_3$ ($x = 0$, 0.04, 0.07 and 0.13) were obtained using a directional solidification method [21]. The average Li content in each crystal was measured by inductive coupled plasma spectroscopy. Crystalline phase identification and lattice parameter measurements were carried out by X-ray diffraction with Cu-K_α radiation using a Rint2000 diffractometer (Rigaku, Tokyo, Japan). Electron transparent specimens were prepared by crushing a slice of each crystal with an agate mortar and pestle and suspending the powder in ethanol, before transferring it to a holey carbon-coated copper grid. Specimens were surface cleaned with an ion cleaner (JIC-410, JEOL, Japan) to remove amorphous surface layers before loading into the electron microscope.

2.2. Transmission electron microscopy

Atomic resolution HAADF and ABF micrographs and SAED patterns were acquired using a JEM-2100F (JEOL) electron microscope equipped with a spherical aberration corrector (CEOS GmbH) and operated at 200 kV. The convergence semiangle in STEM mode was close to 22 mrad, and the collection inner and outer semiangles for the HAADF detector and ABF detector were around 70 and 240 mrad, and 11 and 22 mrad, respectively. SAED simulations were carried out using the xHREM software package (HREM Research Inc.).

Electron energy loss spectroscopy (EELS) data were obtained using a monochromated aberration corrected scanning transmission electron microscope (JEM-2400FCS, JEOL Ltd.) operated at 200 kV equipped with a double Wien filter monochromator and a Gatan Image Filter system (Tridiem ERS, Gatan, Inc.). EELS data were recorded in TEM-ED mode with an energy dispersion of 0.1 eV per channel. The final energy resolution was 300 meV, as determined from the full-width at half-maximum of the zero-loss peak. All background signals in the EELS spectra were subtracted using a power law fitting method.

Atomic resolution energy dispersive spectroscopy (EDS) mapping was performed using a JEM-ARM200CF (JEOL Ltd.) scanning transmission electron microscope operated at 200 kV. The STEM-EDS system was equipped with double solid silicon drift EDS detectors and the solid angle for the whole collection system was about 1.7 sr. The probe size was 1.2 Å with a probe current of about 60 pA.

3. Results

3.1. Average crystal structures and electronic states

The average crystal structure for each composition of LLNbO was determined by XRD. Fig. 2 shows the spectra obtained for all four compositions. All samples were confirmed to be single phase. For Li